



# Effect of Boron on Structural, Optical Characterization of Nanostructured Fe<sub>2</sub>O<sub>3</sub> thin Films

Nagham Yassin Ahmed<sup>1</sup>, Ban A. Bader<sup>2</sup>, Muna Y. Slewa<sup>2</sup>, Nadir Fadhil Habubi<sup>3</sup>, Sami Salman Chiad<sup>3\*</sup>

## Abstract

Fe<sub>2</sub>O<sub>3</sub> thin films were deposited on glass substrate by chemical spray pyrolysis (CSP) technique at a temperature of 450°C. X-Ray diffraction indicates that the films were polycrystalline with a dominant peak along (100). Surface morphology was studied using atomic force microscope (AFM). The grain size values were observed in the zone of (72.46), (71.53) and (59.87) nm for the (Fe<sub>2</sub>O<sub>3</sub>, Fe<sub>2</sub>O<sub>3</sub>:1% B, Fe<sub>2</sub>O<sub>3</sub>:3% B) respectively. Transmittance spectra were recorded to obtain the optical characterizations like absorption edges, which was shifted toward long wavelength. The optical bandgap shows a decrement in their values from (2.65 to 2.45) eV by B doping.

**Key Words:** Fe<sub>2</sub>O<sub>3</sub>: B, Spray Pyrolysis, XRD, AFM, Bandgap.

**DOI Number:** 10.14704/nq.2020.18.6.NQ20183

**NeuroQuantology 2020; 18(6):55-60**

55

## Introduction

Metal oxides have entered many applications like solar cell; photoelectron and electrical devices [1-7]. Iron oxides have diverse shapes like wustite (FeO), magnetite (Fe<sub>3</sub>O<sub>4</sub>), hematite (α-Fe<sub>2</sub>O<sub>3</sub>), and maghemite (γ-Fe<sub>2</sub>O<sub>3</sub>) [8, 9]. Hematite (α-Fe<sub>2</sub>O<sub>3</sub>) is a material with a bandgap of about 2-2.2 eV allowing the absorption of ~40% solar energy via its visible area, due to this factor Fe<sub>2</sub>O<sub>3</sub> is believed as a favorable material for solar energy application [10]. Iron oxide is one of the most famous magnetic materials. Magnetic properties of ferromagnetic and ferrite films were investigated by using the modified second and third order perturbed, gas sensitivity of many materials has been investigated in diverse gases [11-13]. As a sensor, the α-Fe<sub>2</sub>O<sub>3</sub> nanostructures are capable to reveal different gases and vapors like NO<sub>2</sub>, NH<sub>3</sub>, CO, and H<sub>2</sub>S [14-15]. The

high melting point of the metal oxide made the chemical spray pyrolysis technique is suitable method for preparing the metal oxide films [16-19]. This work aims to prepare Fe<sub>2</sub>O<sub>3</sub> and study the impact of B dopant on some physical characterization.

## Experimental

Ferric oxide Fe<sub>2</sub>O<sub>3</sub> thin films were prepared by chemical spray pyrolysis (CSP) method. Fe<sub>2</sub>O<sub>3</sub> films are deposited from 0.1 M of (Fe<sub>2</sub>O<sub>3</sub>Cl<sub>2</sub>) dissolved in redistilled water. The doped material was Boron trichloride (BCl<sub>3</sub>) dissolved in redistilled water, HCl was added as drops to maintain clear solution.

**Corresponding author:** Sami Salman Chiad

**Address:** <sup>1</sup>Department of Medical Instrumentation Techniques Engineering, Electrical Engineering Technical College, Middle Technical University, Iraq; <sup>2</sup>Laser and Photonics Research Center, University of Al-hamdaniya, Nineveh, Iraq; <sup>3</sup>Department of Physics, College of Education, Mustansiriyah University, Iraq.

\*E-mail: dr.sami@uomustansiriyah.edu.iq

**Relevant conflicts of interest/financial disclosures:** The authors declare that the research was conducted in the absence of any commercial or financial relationships that could be construed as a potential conflict of interest.

**Received:** 08 May 2020 **Accepted:** 30 May 2020



The optimal conditions of the deposition was : Glass substrate temperature 450°C, space between nozzle and substrate was 29 cm, spraying period 8 s held by 60 s to prevent cooling, spray average was 4ml/min, and the transporter gas was nitrogen. The structural properties of Fe<sub>2</sub>O<sub>3</sub>: B thin films were carried out employing X-ray diffractometer in 2θ range from 20 to 60. Surface topography of the as deposited films was evaluated by AFM. The UV-Vis spectrophotometer (SHIMADZU Japan) was utilized to gain optical properties.

**Results and Discussion**

Fig. 1 offers XRD pattern of the prepared films. (XRD) show that Fe<sub>2</sub>O<sub>3</sub> and doping with 1% and 3% Fe<sub>2</sub>O<sub>3</sub>: B were polycrystalline with a rhombohedral structure and a dominant peak along (100) direction. These results in agreement with the standard Fe<sub>2</sub>O<sub>3</sub> X-ray diffraction data file [No. 40-1139 JCPDS prevalent].

The average Grain size(D) was obtained from

**Table 1.** Grain size, optical bandgap and structural parameters of the prepared films

Samples	(hk l) Plane	2 θ (°)	FW HM (°)	Grain size (nm)	Optical bandgap (eV)	Dislocations density (× 10 <sup>14</sup> )(lines/m <sup>2</sup> )	Strain × 10 <sup>-4</sup>
Fe <sub>2</sub> O <sub>3</sub> pure	111	31.13	0.62	13.30	2.65	56.5	26.0
Fe <sub>2</sub> O <sub>3</sub> : 1% B	111	30.80	0.58	14.21	2.55	49.5	24.3
Fe <sub>2</sub> O <sub>3</sub> : 3% B	111	30.28	0.55	15.00	2.45	44.4	23.1

highest intensity peaks utilizing Scherrer's equation [20, 21,22]:

$$D = \frac{0.9\lambda}{\beta \cos\theta} \tag{1}$$

Where λ is the wavelength of the X-rays (0.1541 nm), β and θ are (FWHM) and the diffraction angle respectively. The Grain size has been found to vary from 13.30 to 15 nm whereas the strain (%) parameter increased from 26.0 to 23.1, with Au concentration as listed in Table. 1

Other structural parameters such as dislocation density (δ) and strain (ε) are also evaluated. The δ gives number of defects in the films, the values of(δ) and(ε) listed in Table. 1 shows the structural parameters estimated from [23, 24, 25]:

$$\delta = \frac{1}{D^2} \tag{2}$$

$$\epsilon = \frac{\beta \cos\theta}{4} \tag{3}$$

Figure (2) displays the values of FWHM, D, δ and ε via doping content.

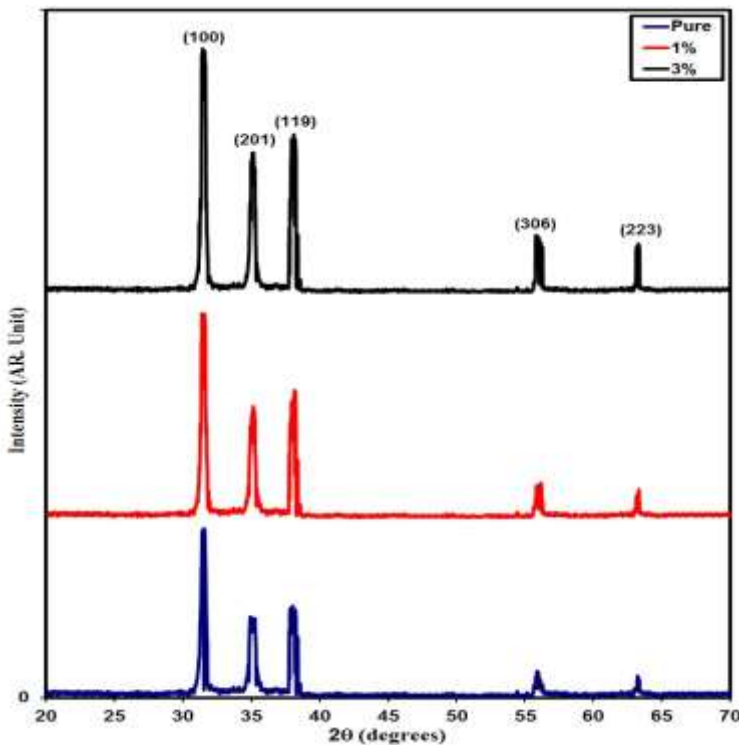


**Fig.1.** XRD-patterns crystalline size of the prepared films



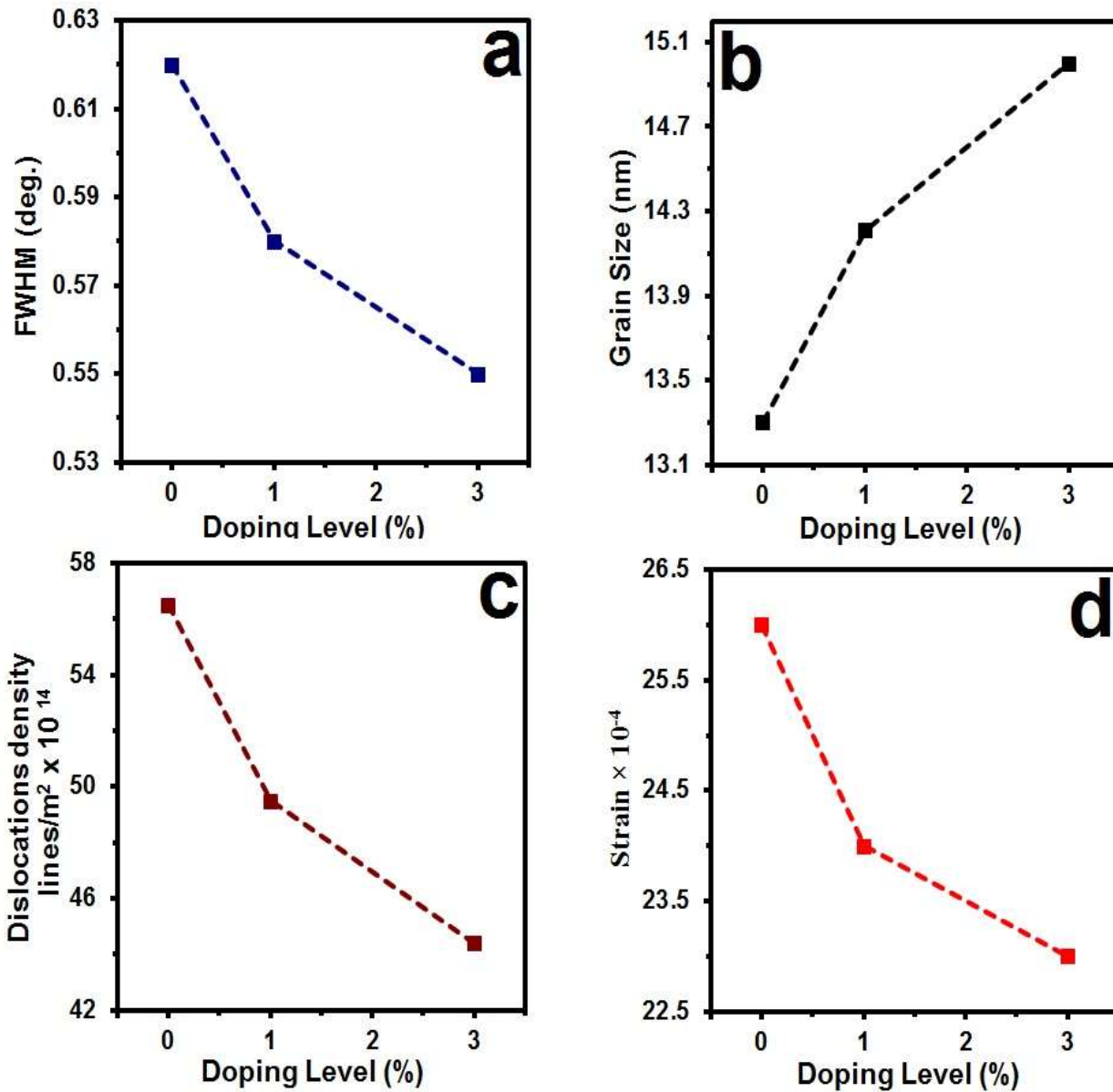


Fig.2. FWHM (a) Grain size (b) Dislocation (c) Strain (d) of the prepared films

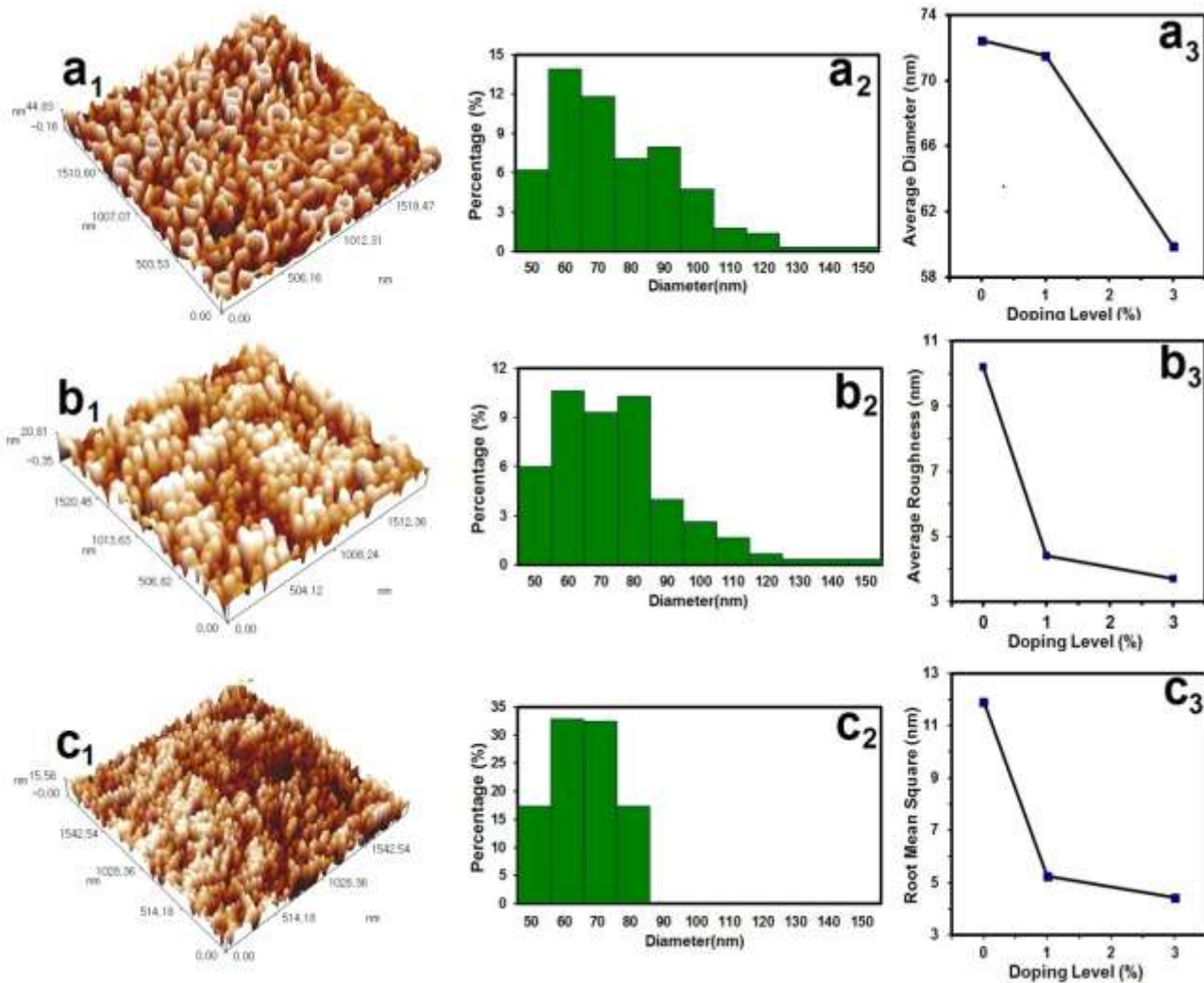
Fig. (3) shows AFM image of three dimensional surface topography of the Fe<sub>2</sub>O<sub>3</sub> films prepared by SPM. The root mean square roughness (R<sub>rms</sub>) and average roughness (R<sub>a</sub>) of prepared films are shown in Table 1. As can be seen, the R<sub>rms</sub> and R<sub>a</sub> follow the doping. The grain size values was in the range of (72.46), (71.53) and (59.87) nm for the

(Fe<sub>2</sub>O<sub>3</sub>, Fe<sub>2</sub>O<sub>3</sub> :1% B, Fe<sub>2</sub>O<sub>3</sub> :3% B) respectively, The R<sub>rms</sub> value of 11.9 nm for as deposited Fe<sub>2</sub>O<sub>3</sub> thin films decreased to 4.43 nm by decreased of doping, R<sub>a</sub> roughness parameters versus dopant content was given in Fig. 3 (a<sub>3</sub>, b<sub>3</sub>, and c<sub>3</sub>) respectively. Table (2) represents the values of AFM parameters.

Table 2. AFM parameters of the deposited films

Samples	Average Particle size nm	Roughness Average (nm)	R <sub>rms</sub> (nm)
Fe <sub>2</sub> O <sub>3</sub>	72.46	10.2	11.9
Fe <sub>2</sub> O <sub>3</sub> : 1% B	71.53	4.40	5.24
Fe <sub>2</sub> O <sub>3</sub> : 1% B	59.87	3.75	4.43





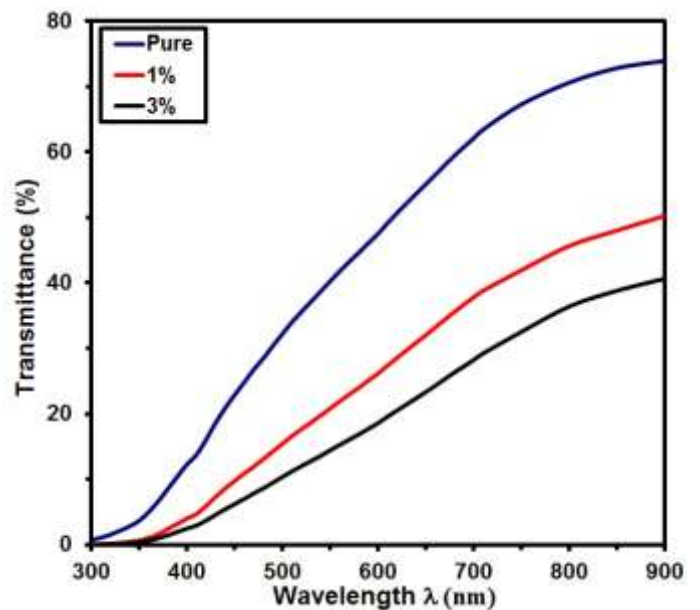
**Fig. 3.** AFM images of the prepared films (a<sub>1</sub>, b<sub>1</sub> and c<sub>1</sub>), granularly distributed (a<sub>2</sub>, b<sub>2</sub> and c<sub>2</sub>) and variation of AFM parameters via doping (a<sub>3</sub>, b<sub>3</sub> and c<sub>3</sub>)

Figure (4) displays transmittance spectra of pure Fe<sub>2</sub>O<sub>3</sub> films for (Fe<sub>2</sub>O<sub>3</sub>:1% B, Fe<sub>2</sub>O<sub>3</sub>:3% B). It is seen that maximum transmittance was 75% for Fe<sub>2</sub>O<sub>3</sub>.

Fig.5 shows the absorption coefficient( $\alpha$ ) decreased with an increase at 1% or 3% doping. The bandgap energy  $E_g$  was estimated from the relation below[26,27]:

$$(\alpha hv) = A(hv - E_g)^{\frac{1}{2}} \quad (4)$$

Where A is the constant,  $hv$  is the photon energy. Figure 6 shows relation of  $(\alpha hv)^2$  vs.  $hv$ . The bandgap of Fe<sub>2</sub>O<sub>3</sub> film for the three films is 2.65, 3.0 and 2.45 eV, respectively. It is clearly observed that with decrease of films, the optical bandgap was found to be decreased with doping content



**Fig.4.** Transmittance for the prepared films.



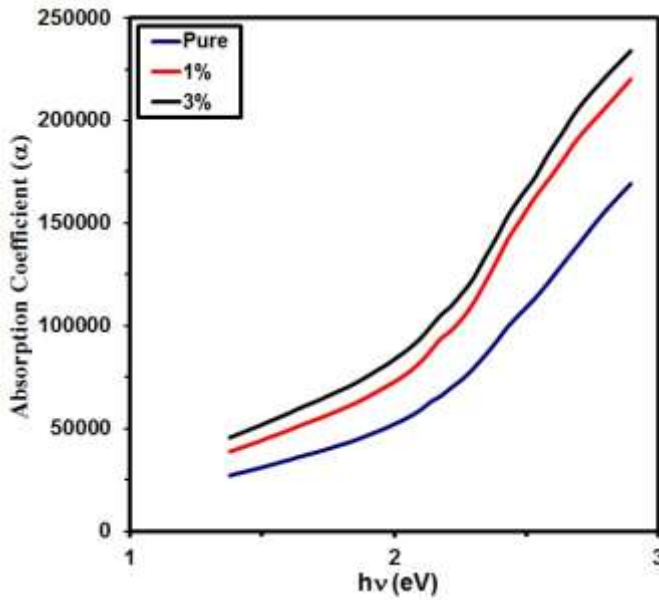


Fig. 5.  $\alpha$  Vshv of the prepared thin films

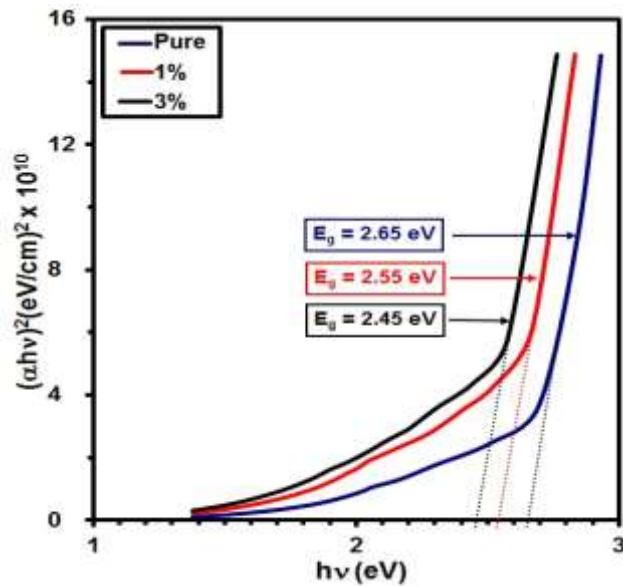


Fig. 6.  $(\alpha hv)^2$  Vshv of the prepared thin films

### Conclusion

Fe<sub>2</sub>O<sub>3</sub> films are prepared under various B dopants, The structure was rhombohedral with a preferred peak in (100). Surface morphology of the prepared films was studied using atomic force microscope (AFM). The grain size was in the zone of (72.46), (71.53) and (59.87) nm for the (Fe<sub>2</sub>O<sub>3</sub>, Fe<sub>2</sub>O<sub>3</sub>:1% B, Fe<sub>2</sub>O<sub>3</sub>:3% B) respectively.

### Acknowledgments

Authors like to appreciate Mustansiriyah University for their efforts in this work.

### References

Shinde SS, Bansode RA, Bhosale CH, Rajpure KY. Physical properties of hematite  $\alpha$ -Fe<sub>2</sub>O<sub>3</sub> thin films: application to photoelectrochemical solar cells. *Journal of Semiconductors* 2011; 32(1): 013001.

Abass KH, Latif DM. The Urbach Energy and Dispersion Parameters dependence of Substrate Temperature of CdO Thin Films Prepared by Chemical Spray Pyrolysis. *International Journal of ChemTech Research* 2016; 9(9): 332-338.

Abass KH, Shinen MH, Alkaim AF. Preparation of TiO<sub>2</sub> Nanolayers via Sol-Gel Method and Study the Optoelectronic Properties as Solar Cell Application. *Journal of Engineering and Applied Sciences* 2018; 13(22): 9631-9637.

Abass KH, Mohammed MK. Fabrication of ZnO: Al/Si Solar Cell and Enhancement its Efficiency Via Al-Doping. *Nano Biomed. Eng.*, 2019; 11(2): 170-177.

Abass KH, Obaid NH. 0.006 wt.% Ag-Doped Sb<sub>2</sub>O<sub>3</sub> Nanofilms with Various Thickness: Morphological and optical properties. In *Journal of Physics: Conference Series* 2019; 1294(2): 022005.

Muhammad SK, Hassan ES, Qader KY, Abass KH, Chiad SS, Habubi NF. Effect of Vanadium on Structure and Morphology of SnO<sub>2</sub> Thin Films. *Nano Biomed. Eng.*, 2020; 12(1): 67-74.

Tuama AN, Abbas KH, Hamzah MQ, Oudah S. An Overview on Characterization of Silver/Cuprous Oxide Nanometallic (Ag/Cu<sub>2</sub>O) As Visible Light Photocatalytic. *International Journal of Advanced Science and Technology* 2019; 29(3): 5008 - 5018.

Al-Kuhaili MF, Saleem M, Durrani SMA. Optical properties of iron oxide ( $\alpha$ -Fe<sub>2</sub>O<sub>3</sub>) thin films deposited by the reactive evaporation of iron. *Journal of alloys and compounds* 2012; 521: 178-182.

Mansour H, Letifi H, Bargougui R, De Almeida-Didry S, Negulescu B, Autret-Lambert C, Ammar S. Structural, optical, magnetic and electrical properties of hematite ( $\alpha$ -Fe<sub>2</sub>O<sub>3</sub>) nanoparticles synthesized by two methods: polyol and precipitation. *Applied Physics A* 2017; 123(12): 787.

Ismail RA, Najim Y, Ouda M. Spray Pyrolysis Deposition of  $\alpha$ -Fe<sub>2</sub>O<sub>3</sub> Thin Film. *e-Journal of Surface Science and Nanotechnology* 2008; 6: 96-98.

Samarasekara P, Saparamadu U. Investigation of Spin Reorientation in Nickel Ferrite Films. *Georgian electronic scientific journals: Physics* 2012; 1(7) :15-20.

Samarasekara P, Gunawardhane NHPM. Explanation of easy axis orientation of ferromagnetic films using Heisenberg Hamiltonian. *Georgian electronic scientific journals: Physics* 2011; 2(6) :62-69.

Samarasekara P. Influence of third order perturbation on Heisenberg Hamiltonian of thick ferromagnetic films. *Electronic Journal of Theoretical Physics* 2008; 5(17): 227-236.

Huo L, Li Q, Zhao H, Yu L, Gao S, Zhao J. Sol-gel route to pseudocubic shaped  $\alpha$ -Fe<sub>2</sub>O<sub>3</sub> alcohol sensor: preparation and characterization. *Sensors and Actuators B: Chemical* 2005; 107(2): 915-920.

Balouria V, Kumar A, Samanta S, Singh A, Debnath AK, Mahajan A, Gupta SK. Nano-crystalline Fe<sub>2</sub>O<sub>3</sub> thin films for ppm



- level detection of H<sub>2</sub>S. Sensors and Actuators B: Chemical 2013; 181: 471-478.
- Oday MA, Firas SA, Haider AK, Mohammed OD, Khalid HA, Nadir FH, Sami SC. Influence of Bismuth Dopant on Physical Properties of nanostructured TiO<sub>2</sub> Thin Films. Test Engineering and Management 2020; 83: 11142-11147.
- Ali MJ, Akeel SA, Reem SA, Nadir FH, Khalid HA, Sami SC. Effect of Bismuth Addition on Thin Films of ZNO on Structure and Optical Properties. Test Engineering and Management 2020; 83: 11125-11132.
- Firdous SA, Nagham YA, Reem SA, Nadir FH, Khalid HA, Sami SC. Effects of Substrate Type on Some Optical and Dispersion Properties of Sprayed CdO Thin Films. NeuroQuantology 2020; 18(3): 56-65.
- Reem SA, Khansaa SS, Ali MJ, Sami SC, Khalid HA, Nadir FH. Characterization of ZnO Thin Film/p-Si Fabricated by Vacuum Evaporation Method for Solar Cell Applications. NeuroQuantology 2020; 18(1): 26-31.
- Dawood MO, Chiad SS, Ghazai AJ, Habubi NF, Abdulmunem OM. Effect of Li doping on structure and optical properties of NiO nano thin-films by SPT. In AIP Conference Proceedings 2020; 2213(1): 020102.
- Reem SA, Khansaa SS, Muhammad HA, Khalid HA, Nadir FH, Ismaeel AA, Sami SC. Enhancement of CdO Film Via Li Additive: Structural and Optical Properties. Test Engineering and Management 2020; 83: 11148 - 11153.
- Sami SC, Tahseen HM. The effect of Ti on physical properties of Fe<sub>2</sub>O<sub>3</sub> thin films for gas sensor applications. International Journal of Nanoelectronics and Materials, Malaysia 2020; 13(2): 221-232.
- Hassan ES, Mubarak TH, Chiad SS, Habubi NF, Khadayeir AA, Dawood MO, Al-Baidhany IA. Physical Properties of indium doped Cadmium sulfide thin films prepared by (SPT). In Journal of Physics: Conference Series 2019; 1294(2): 022008.
- Jandow NN, Habubi NF, Chiad SS, Al-Baidhany IA, Qaeed MA. Annealing Effects on Band Tail Width, Urbach Energy and Optical Parameters of Fe<sub>2</sub>O<sub>3</sub>:Ni Thin Films Prepared by Chemical Spray Pyrolysis Technique. International Journal of Nanoelectronics and Materials 2019; 12(1): 1-10.
- Ehssan SH, Abdulhussain KE, Suzan HM, Mohammed HS, Sami SC. Silver oxides nanoparticle in gas sensors applications. Journal of Materials Science: Materials in Electronics, Netherlands 2019: 1-9.
- Duha MAL, Sami SC, Muhssen SE, Khalid HA, Nadir FH, Hadi AH. Dispersion Parameters of Polyvinyl Alcohol Films doped with Fe, IOP Conf. Series: Journal of Physics: Conf. Series, United Kingdom 2018; 1003: 012094.
- Nadir FH, Khalid HA, Chiad SS, Duha MAL, Jandow NN. A Ismaeel Al Baidhany, Effects of FeCl<sub>3</sub> additives on optical parameters of PVA, IOP Conf. Series: Journal of Physics: Conf. Series, United Kingdom 2018; 1003: 012108.

